

## **RADIOFREQUENCY PERFORMANCES OF TRANSPARENT ULTRA-WIDEBAND ANTENNAS**

**J. Hautcoeur<sup>1,2</sup>, F. Colombel<sup>1,\*</sup>, X. Castel<sup>1</sup>, M. Himdi<sup>1</sup>, and E. Motta-Cruz<sup>2</sup>**

<sup>1</sup>Institut d'Electronique et de Télécommunications de Rennes, UMR-CNRS 6164, Université de Rennes 1, 18, rue Henri Wallon 22004 SAINT-BRIEUC and Campus de Beaulieu, 263 av. G<sup>al</sup> Leclerc, RENNES Cedex 35042, France

<sup>2</sup>Bouygues Telecom, 76 rue des Français Libres, NANTES 44263, France

**Abstract**—In this paper, optically transparent ultra-wideband (UWB) monopole antennas in S-band and Cband are presented, compared and discussed. Three transparent UWB antennas elaborated from the AgGL (Silver Grid Layer) material with various levels of transparency (54.5%, 73.4% and 80.3%) and of sheet resistances  $0.018 \Omega/\text{sq}$ ,  $0.022 \Omega/\text{sq}$  and  $0.052 \Omega/\text{sq}$ , respectively are tested. The radiofrequency measurements show performances very close to those of a light reflecting reference antenna made of a continuous silver/titanium bilayer ( $0.0026 \Omega/\text{sq}$  sheet resistance). Conversely, the fourth transparent antenna, made of usual transparent conducting oxide/metal multilayer presents significant ohmic losses and weak radiofrequency performances. The gains of the UWB AgGL antennas are similar to that of the reference antenna ( $\sim 6$  dBi max.). Whereas the gain of the transparent multilayer antenna always stays  $\sim 2$  dB lower than that of the reference. This work demonstrates the relevance of AgGL coating in the fabrication of transparent UWB antennas with high radiation efficiency.

---

*Received 26 May 2011, Accepted 11 July 2011, Scheduled 20 July 2011*

\* Corresponding author: Franck Colombel (franck.colombel@univ-rennes1.fr).

## 1. INTRODUCTION

During the last ten years, with the progress of wireless communications and the increase of radio applications like GPS, UMTS, Bluetooth, WLAN, etc. antennas with soft visual impact became an attractive solution to optimize their integration in the critical areas such as historical city center, shops, etc. Furthermore, ultra-wideband application is a promising solution for future short-range wireless communications with high data rates as well as radar and localization. First reports on transparent antennas have been published in the early 90s [1, 2]. More recent studies promote this research. For example in [3], Turpin and Baktur studied the development of transparent antennas on solar cells, and in [4] Song et al. propose a method that improves the efficiency of transparent antennas based on the commercial available AgHT films (silver coated polyester films). This last contribution demonstrates the poor electrical properties of available transparent and conductive materials due to high sheet resistances. This is also demonstrated in [5], where Katsounaros et al. present a transparent antenna for ultra-wideband (UWB) applications. The material used to achieve this antenna is also the commercial AgHT-4 film.

Commercially available films and transparent conducting multilayers are based on ultrathin metal film (silver (Ag), copper (Cu) or aluminum (Al)) sandwiched between transparent conducting oxide (TCO) layers like indium tin oxide (ITO) or fluorine-doped tin oxide (FTO). Optical transmittance of samples at a specified wavelength is defined as the ratio between the intensity of the light coming out of the sample and the intensity of the incident light. In this paper, the ratio is given as a percentage. Although the maximum optical transmittance values of both materials are quite high and close to 75% at a specific wavelength in the visible light spectrum from 400 nm to 800 nm, the minimum sheet resistance ( $R_s$ ) of multilayers is equal to  $1.2 \Omega/\text{sq}$  [6] and to  $4.5 \Omega/\text{sq}$  for the commercial AgHT-4 film. In [5], it is shown that an aluminum layer is around 30 times more conductive than the AgHT-4 film. This leads to a 5 dB gain loss of the AgHT-4 antenna. For an industrial point of view and for large amounts of products, thin film process like RF sputtering technique coupled to photolithography and wet etching can be used for AgGL products. The over expense of this technology for transparent antenna will be balanced by the expected increasing cost of indium and the weak radiofrequency performances of the commercially available transparent and conductive film.

The aim of this paper is to present optically transparent UWB monopole antennas based on AgGL (Ag Grid Layer) coating, which

provide radiofrequency performances identical to those of pure metal reference antenna. In the first part, three transparent UWB monopole antennas elaborated from AgGL with various optical transparencies and sheet resistances are described. In the second part, we studied the radiofrequency performances of the AgGL antennas. Then, they are compared to those of a home-made ITO/Ag/ITO multilayer antenna [7] which stands for the state of the art in transparent antenna, and of a light reflecting silver/titanium antenna which stands for the radiofrequency performances. Identical design is used for all antennas. In the third part, we increase the overall transparency of the UWB monopole antennas by optimizing the design. At the end, we discuss the limits of the new AgGL coating and give criteria to achieve transparent antennas with high radiation efficiency.

## 2. ULTRA-WIDEBAND ANTENNA DESIGN

We have fabricated five ultra-wideband monopole antennas. Each antenna is printed on a 50 mm  $\times$  50 mm, 1.1 mm-thick 1737 Corning glass substrate (relative dielectric permittivity  $\epsilon_r = 5.7$  and loss angle  $\tan \delta = 0.006$  at 2 GHz). The antenna under test is placed perpendicularly above a 300 mm  $\times$  300 mm ground plane, and directly fed by a coaxial probe. The antenna layout dimensions are also indicated in Figure 1. The transparent antennas, namely UWB-1, UWB-2 and UWB-3, are fabricated from the AgGL material: a meshed metal bilayer [8]. This transparent and conductive coating is elaborated from a 6  $\mu\text{m}$ -thick silver (Ag) film grown by RF sputtering

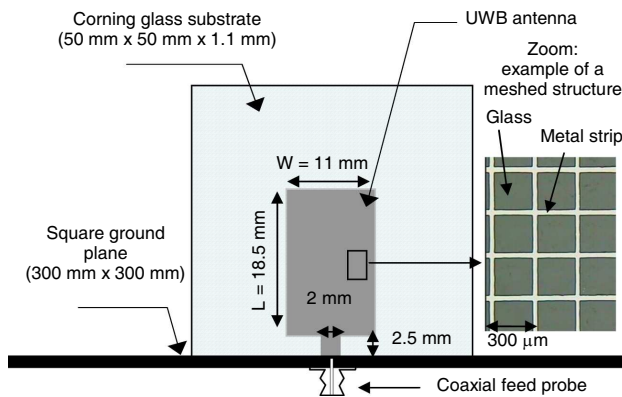


**Figure 1.** Structure and layout dimensions of the ultra-wideband antenna.

on a 5 nm ultrathin adhesion titanium (Ti) underlayer. A periodic array of square apertures is achieved in the metal bilayer by standard photolithographic wet etching process. More details are reported in [8]. In [9], the 50 mm  $\times$  50 mm transparent lozenge antenna was achieved by the use of a mesh pitch of 300  $\mu\text{m}$  and a metal strip close to 20  $\mu\text{m}$ . A standard four-point probe configuration gave a 0.054  $\Omega/\text{sq}$  measured sheet resistance  $R_s$ . In this study, the metal strip is also close to 20  $\mu\text{m}$  but we used three different mesh pitches: 100  $\mu\text{m}$ , 200  $\mu\text{m}$  and 300  $\mu\text{m}$  for UWB-1, UWB-2 and UWB-3 antennas, respectively. With these parameters, the said antennas have measured the sheet resistances equal to 0.018  $\Omega/\text{sq}$ , 0.022  $\Omega/\text{sq}$  and 0.052  $\Omega/\text{sq}$  respectively. Another ultrawideband transparent antenna has been elaborated from a homemade 200 nm thick ITO/Ag/ITO multilayer. This sample will stand for the state of the art for usual transparent and conductive layers with a measured sheet resistance of 5.0  $\Omega/\text{sq}$  [7]. The last antenna, made from a continuous 6  $\mu\text{m}/5$  nm-thick Ag/Ti bilayer ( $R_s = 0.0026$   $\Omega/\text{sq}$ ) is a light reflecting antenna which stands for the reference from a radioelectrical behaviour point of view. Optical transmittance (T) of samples has been recorded with a UV/Visible spectrophotometer in the spectral range 200–1100 nm as shown in Figure 2. For the UWB-1, UWB-2 and UWB-3 antennas, measured transmittances remain constant over the whole visible light spectrum and are equal to 54.5%, 73.4% and 80.3% respectively. For the ITO/Ag/ITO multilayer antenna, the measured transmittance varies and ranges from 37% to

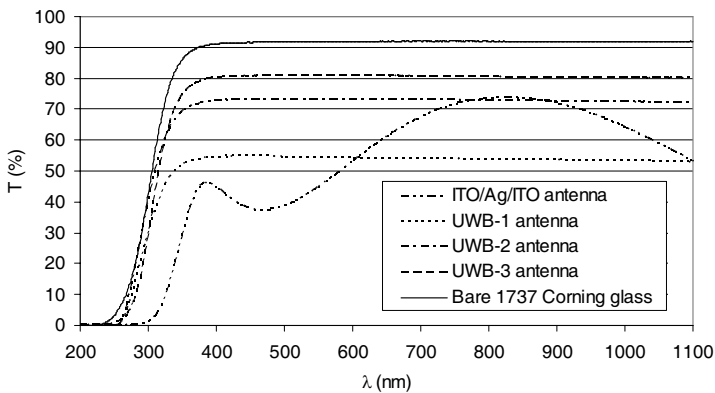


**Figure 2.** Transmission spectra of the four transparent UWB antennas: three based on AgGL coating and one on ITO/Ag/ITO multilayer. Spectrum of a bare Corning glass is also plotted for a comparison.

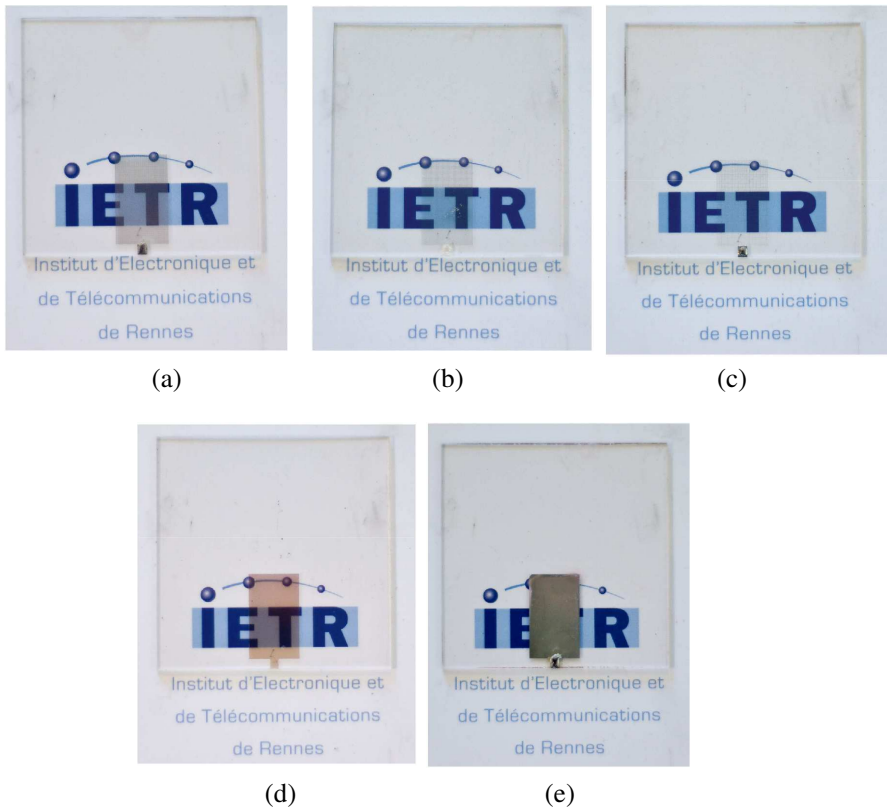


**Figure 3.** UWB antennas printed on Corning glass substrates. (a)–(c) UWB-1, UWB-2 and UWB-3 AgGL antennas ( $T = 54.5\%$ ,  $73.4\%$  and  $80.3\%$ , respectively); (d) ITO/Ag/ITO multilayer antenna ( $37\% < T < 74\%$ ); (e) Light reflecting reference antenna.

$74\%$  in the visible light spectrum due to interference fringes. Note that all transmittance values include Fresnel losses. Physical characteristics of the antennas are reported in Table 1. The five UWB antennas are also displayed in Figure 3.

### 3. ANTENNA MEASUREMENTS

#### 3.1. Input impedances

Input impedances have been measured between 2 GHz and 6 GHz. In Figure 4, the measured input impedances of the UWB-1 AgGL antenna and of the reference antenna have been compared with the simulation

**Table 1.** Electrical and optical antenna characteristics.

Antenna	Measured sheet resistance $R_s$ ( $\Omega/\text{sq}$ )	Measured transparency in visible light spectrum (%)
UWB-1	0.018	54.5
UWB-2	0.022	73.4
UWB-3	0.052	80.3
ITO/Ag/ITO multilayer	5.0	$37 < T < 74$
Continuous Ag/Ti (reference)	0.0026	0

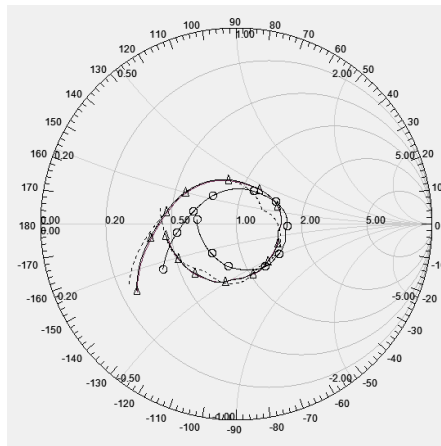


**Figure 4.** Theoretical and measured input impedances between 2 GHz and 6 GHz:  $\Delta\Delta\Delta$ : UWB-1 AgGL antenna ( $R_s = 0.018 \Omega/\text{sq}$ ,  $T = 54.5\%$ );  $\circ\circ\circ$ : ITO/Ag/ITO multilayer antenna ( $R_s = 5.0 \Omega/\text{sq}$ ,  $37\% < T < 74\%$ ); - - -: Simulation (HFSS); —: reference antenna ( $R_s = 0.0026 \Omega/\text{sq}$ ,  $T = 0\%$ ).

results (HFSS<sup>TM</sup>) of a non-meshed reference antenna. They agree fairly well and fit strongly with the theoretical results. The input impedance of the ITO/Ag/ITO multilayer antenna is also presented in Figure 4. As expected, it is more resistive due to its higher sheet resistance. These first results highlight the possibility to design an UWB meshed-metal antenna equivalent to a continuous metal counterpart, unlike usual transparent and conductive multilayer.

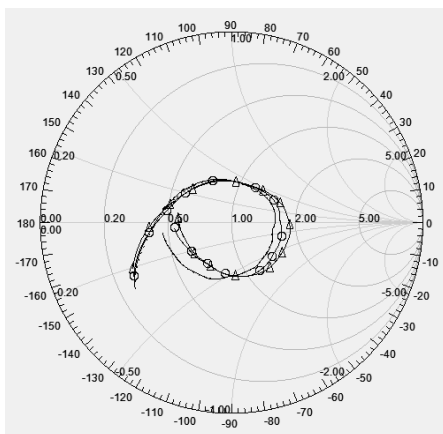


**Figure 5.** Measured input impedances between 2 GHz and 6 GHz: —: UWB-1 AgGL antenna ( $R_s = 0.018 \Omega/\text{sq}$ ,  $T = 54.5\%$ ); ooo: UWB-2 AgGL antenna ( $R_s = 0.022 \Omega/\text{sq}$ ,  $T = 73.4\%$ );  $\Delta\Delta\Delta$ : UWB-3 AgGL antenna ( $R_s = 0.052 \Omega/\text{sq}$ ,  $T = 80.3\%$ ). - - -: reference antenna ( $R_s = 0.0026 \Omega/\text{sq}$ ,  $T = 0\%$ ).

In Figure 5, the input impedances of the UWB-1, UWB-2 and UWB-3 AgGL antennas are compared to that of the reference antenna. Beyond 2 GHz, the higher the transparency of AgGL antenna (from 54.5% to 80.3%), the higher is the shift with the reference input impedance. It is underlined in Figure 6 where the reflection coefficients  $S_{11}$  of the AgGL antennas are presented. First, the response of the UWB-1 antenna for a pitch of  $100 \mu\text{m}$  fits strongly with that of the reference antenna. But, when the pitch of the mesh increases to  $200 \mu\text{m}$  for the UWB-2 antenna and  $300 \mu\text{m}$  for the UWB-3 antenna, the divergence of return loss increases. We assume that this phenomenon is due to the edges of meshed antennas, which are not perfectly defined. This point will be discussed in the last part of this study. Nevertheless, the reflection coefficients of the UWB-2 and UWB-3 antennas remain lower than  $-10 \text{ dB}$ .

### 3.2. Antenna Gains

Radiation patterns of these five UWB antennas are similar to those of a typical monopole antenna. The total gains, between 2 GHz and 6 GHz, of the UWB-1 AgGL antenna, the ITO/Ag/ITO multilayer antenna and of the reference counterpart are gathered in Figure 7. They are compared with the simulation results. Gains of the UWB-1

AgGL antenna and of the reference antenna overlap perfectly. These results also fit well with the theoretical values. In contrast, the gain of the multilayer antenna is always lower about 2 dB. This is due to both ITO/Ag/ITO ohmic loss ( $R_s = 5.0 \Omega/\text{sq}$ ) and skin depth effect [7]. Indeed at 2 GHz and at 6 GHz, the skin depth is equal to  $11.2 \mu\text{m}$  and

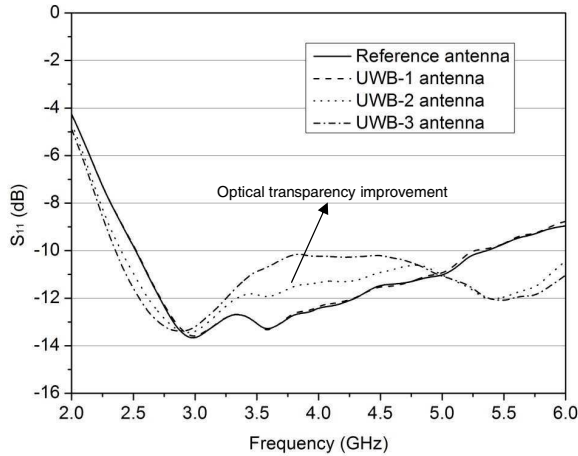


**Figure 6.** Reflection coefficients vs. frequency of the UWB-1, UWB-2 and UWB-3 AgGL antennas and of the reference antenna. Influence of the optical transparency improvement by pitch increasing.

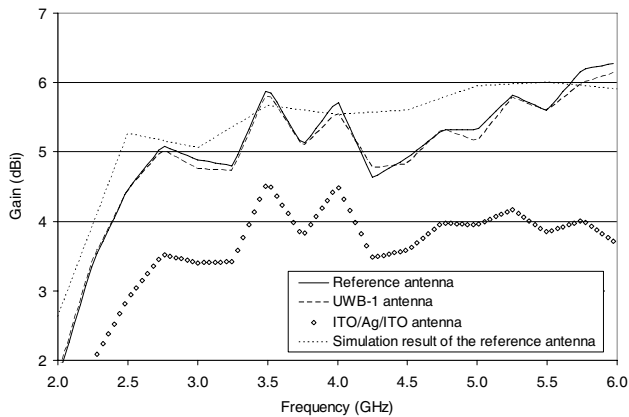


**Figure 7.** Measurements of total gain vs. frequency of the UWB-1 AgGL antenna; the ITO/Ag/ITO multilayer antenna and the reference antenna. Comparison with the simulation results.



6.5  $\mu\text{m}$ , respectively. Note that the skin depth of the metal bilayer is equal to 1.4  $\mu\text{m}$  and 0.8  $\mu\text{m}$  respectively at the same frequency band. For a better understanding, we have calculated the efficiency of the antennas measured in Figure 7. The efficiency has been evaluated for those antennas with the theoretical directivity and the measured gain between 2.5 and 5 GHz where the antennas are well matched. Taking into account the variation of the measured gain, we found that the efficiency is varying between 80% and 90% for UWB-1 and the reference antenna. For a clear presentation, the gains of the UWB-2 and UWB-3 AgGL antennas are not presented in Figure 7, because they are just a few tenth of dB lower than the reference gain. These results demonstrate the increase of the transparency through a pitch increment up to 300  $\mu\text{m}$  which has non-significant effect on the meshed antenna gain.

### 3.3. Optimization of the Transparency

In order to improve the overall transparency of the transparent UWB AgGL antennas, two rectangular openings have been added in the antenna design. Dimensions of the said openings are given in Figure 8. So, a new reference antenna and three new UWB AgGL antennas, namely UWB-4, UWB-5 and UWB-6 have been fabricated as shown in Figure 9. The UWB-4, UWB-5 and UWB-6 AgGL antennas have the same dimensions of the metal strip and mesh pitches as that of the previous UWB-1, UWB-2 and UWB-3 AgGL antennas respectively. So the local measured transparencies of the meshed samples are identical but with the help of the openings, the overall transparency of the

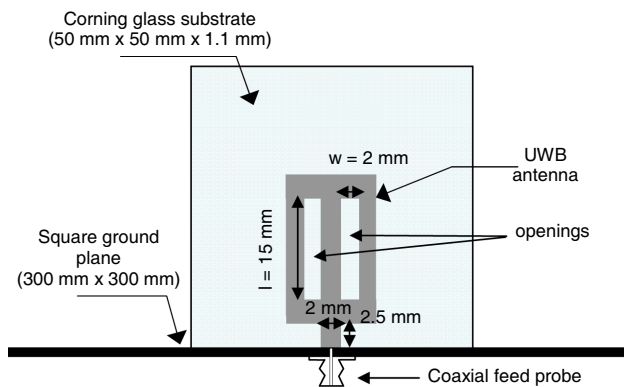


**Figure 8.** Structure of the ultra-wideband antenna with two additional openings. Their dimensions ( $l, w$ ) are given in figure.

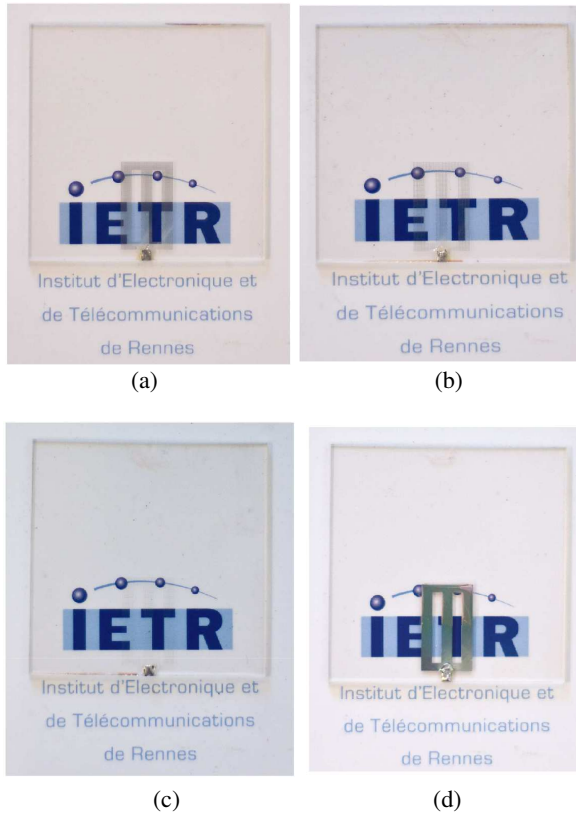


**Figure 9.** UWB antennas with openings, printed on 1737 Corning glass substrates: (a)–(c) UWB-4, UWB-5 and UWB-6 AgGL antennas ( $T = 54.5\%$ ,  $73.4\%$  et  $80.3\%$ , respectively); (d) Reference antenna.

meshed antennas is improved. The measured sheet resistances and the gains are also the same as those of the UWB-1, UWB-2 and UWB-3 antennas as shown in Figure 7. In Figure 10, the measured reflection coefficient of the three UWB AgGL antennas between 2 GHz and 6 GHz is compared with that of the reference antenna. We noticed a significant modification of the  $S_{11}$  when the transparency of the antenna changes due to the increase of the pitch. This is due to a technological restriction of the AgGL coating during the elaboration step. Indeed the edges of the meshed patterns are not perfectly defined on the photomask used in photolithographic process [8]. As a result, the radioelectrical size of the antenna is altered of one pitch on each inner and outer side, as described in Figure 11. And the modification of the antenna dimension (size reduction) is particularly significant when

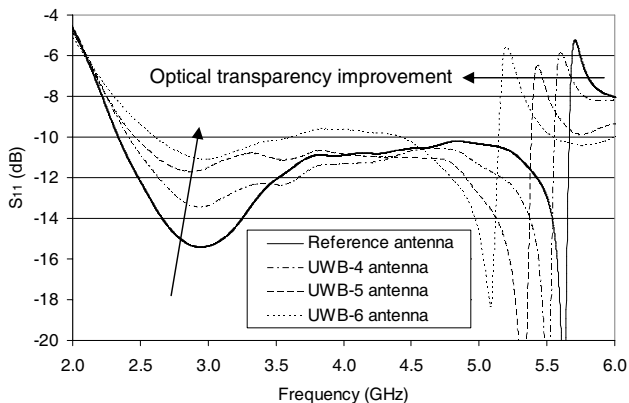


**Figure 10.** Reflection coefficients vs. frequency of the UWB-4, UWB-5 and UWB-6 AgGL antennas and of the reference antenna (structure with apertures). Influence of the optical transparency improvement by pitch increasing.

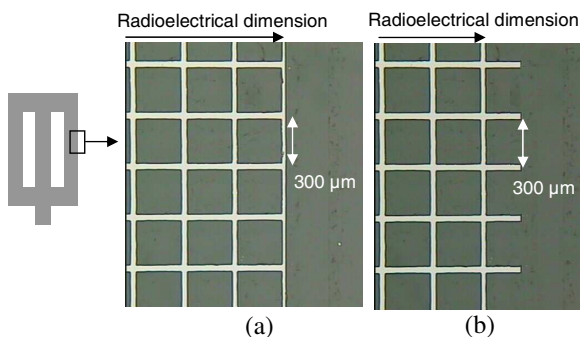


**Figure 11.** Edge of an AgGL antenna (300 μm-pitch). (a) Edge closed by a metal strip; (b) open edge.

a large pitch is used. To verify this assumption, a numerical study has been performed using HFSS<sup>TM</sup>. Due to the values of wavelengths as 150 mm and 50 mm in free space between 2 and 6 GHz and the width of the metal strip as 20 μm used in the meshed antennas, the required computing power is too high. So, three non-meshed antennas with openings have been simulated after removing each edge of pitch values: 100 μm, 200 μm or 300 μm. The fourth simulated antenna is the referred one with the rigorous dimensions as shown in Figure 8. The simulated reflection coefficients are presented in Figure 12. We noticed a similar behaviour as observed in Figure 10.

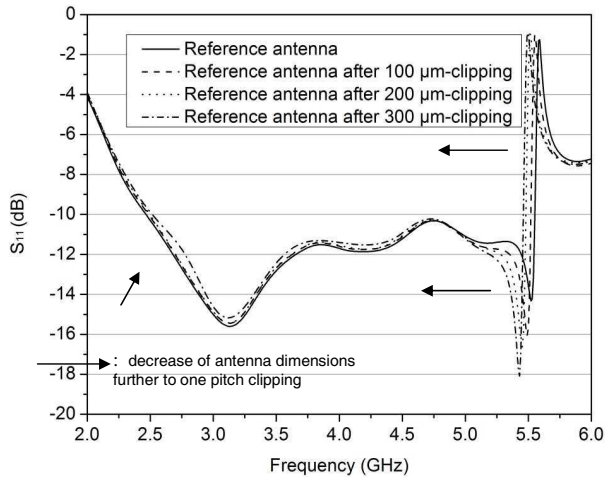


**Figure 12.** Evolution of reflection coefficients vs. frequency further to one pitch clipping.

So, these results demonstrate the impact of photomask quality. Each edge of AgGL antennas must be bordered by a metal strip in order to reach the expected radiofrequency performances.

#### 4. CONCLUSION

Various transparent monopole antennas for ultra-wideband applications in S-band and C-band have been designed and fabricated on 1737 Corning glass substrates, and their radiofrequency performances was studied and explained. The transparent antenna elaborated from ITO/Ag/ITO multilayer shows detrimental ohmic loss and skin depth effect, which impact directly on its gain value ( $\sim 4.5$  dBi max.). Besides, the transparent antennas based on the AgGL coating show a gain of  $\sim 6$  dBi max which is the same as light reflecting antenna made from a continuous Ag/Ti bilayer and standing for the reference. Input impedances, return loss and gains of the AgGL antenna fabricated from the narrower mesh (pitch of  $100\ \mu\text{m}$ ) and of the reference counterpart fit strongly with the simulation results (HFSS<sup>TM</sup>). This demonstrates the opportunity to design transparent antennas for UWB applications without affecting the radiofrequency performances. Nevertheless, a restriction of the AgGL material has been observed with a reduction in the impedance bandwidth for a larger mesh of pitch  $300\ \mu\text{m}$ . This restriction should be removed by bordering each edge of the meshed antenna with a metal strip.

## REFERENCES

1. Ito, K. and M. Wu, "See-through microstrip antennas constructed on a transparent substrate," *7th International Conference on Antennas and Propagation Proceedings*, 133–136, York, UK, 1991.
2. Wu, M. and K. Ito, "Basic study on see-through microstrip antennas constructed on a window glass," *Antennas and Propagation Society International Symposium Proceedings*, 499–502, Chicago, USA, 1992.
3. Turpin, T. W. and R. Baktur, "Meshed patch antenna integrated on solar cell," *IEEE Antennas and Wireless Propagation Letters*, Vol. 8, 693–696, 2009.
4. Song, H. J., T. Y. Hsu, D. F. Sievenpiper, H. P. Hsu, J. Schaffner, and E. Yasan, "A method for improving the efficiency of transparent film antennas," *IEEE Antennas and Wireless Propagation Letters*, Vol. 7, 753–756, 2008.
5. Katsounaros, A., Y. Hao, N. Collings, and W. A. Crossland, "Optically transparent antenna for ultra wide-band applications," *3rd European Conference on Antennas and Propagation*, 1918–1921, Berlin, Germany, 2009.
6. Klöppel, A., B. Meyer, and J. Trube, "Influence of substrate temperature and sputtering atmosphere on electrical and optical properties of double silver layer systems," *Thin Solid Films*, Vol. 392, 311–314, 2001.
7. Colombel, F., X. Castel, M. Himdi, G. Legeay, S. Vigneron, and E. Motta Cruz, "Ultrathin metal layer, ITO film and ITO/Cu/ITO multilayer towards transparent antenna," *IET Science, Measurement and Technology*, Vol. 3, 229–234, 2009.
8. Hautcoeur, J., X. Castel, F. Colombel, R. Benzerga, M. Himdi, G. Legeay, and E. Motta Cruz, "Transparency and electrical properties of meshed metal films," *Thin Solid Films*, Vol. 519, 3851–3858, 2011.
9. Hautcoeur, J., F. Colombel, X. Castel, M. Himdi, and E. Motta Cruz, "Optically transparent monopole antenna with high radiation efficiency manufactured with a silver grid layer (AgGL)," *Electronics Letters*, Vol. 45, 1014–1015, 2009.